UNITED STATES DEPARTMENT OF THE INTERIOR

GEOLOGICAL SURVEY

Aeromagnetic Map and Interpretation of Magnetic and Gravity Data, Circle Quadrangle, Alaska

Open-File Report 83-170-C

by

John W. Cady[1] and Florence R. Weber[2]

[1]Denver, Colorado

[2]Fairbanks, Alaska

1983

TABLE OF CONTENTS

TABLES

FIGURES

PLATES

INTRODUCTION

The aeromagnetic map of Circle quadrangle reflects the distribution of magnetic minerals in the upper few kilometers of the crust. The map is dominated by elongate highs and lows caused by lithologic units exposed at the surface for considerable distances along strike. Buried magnetic sources occur mainly within the Tintina fault zone and Yukon Flats. Major geophysical terranes are delineated by discontinuities in the pattern of magnetic anomalies and changes in the mean Bouguer gravity anomaly.

The aeromagnetic map provides an essential tool for geologic mapping in Circle quadrangle. Outcrop exposures are commonly poor and discontinuous, and the elongate magnetic anomalies indicate that lithologic units have greater continuity along strike than can readily be observed by the geologist in the field.

A preliminary aeromagnetic interpretation should be made prior to beginning geologic field work. A good interpretation will contain multiple hypotheses that can be tested by geologic fieldwork. Aeromagnetic maps at a scale of 1:63,360 can be used to plan initial geologic traverses that cross strike. A magnetic susceptibility meter about twice the size of a Brunton compass is useful for determining which rocks are magnetic. Once magnetic marker units have been identified, they can be located along strike using the 1:63,360 aeromagnetic maps as a guide.

The geologist using aeromagnetic maps to guide field work in an area like the Circle quadrangle must be prepared for disappointments. In greenschist-facies metamorphic terranes magnetic anomalies are commonly caused by easily eroded chloritic schist that underlies tundra-covered swales. A portable magnetometer, either hand-held or towed by helicopter, is a useful tool for establishing whether magnetic rocks occur beneath a swale. In southwestern Circle quadrangle, many of the ridges are composed of resistant quartzite. A brushy trek off the ridge may be required to locate the source of a magnetic high. On the bright side, once the geologist has established that a recessive, magnetic unit causes an elongate magnetic high, he may suddenly perceive stratigraphic and (or) compositional layering revealed in an alinement of swales.

It is helpful if the geophysical interpretation and the field geology are done by the same person. When a hypothesis fails, it is more productive if the field geologist can propose and begin to test a new hypothesis to explain a magnetic anomaly, than to simply report back to the geophysicist that his interpretation was wrong.

This interpretation of aeromagnetic and gravity data is part of the AMRAP (Alaska Mineral Resources Assessment Program) folio of Circle quadrangle. The aeromagnetic map (plate 1) was flown and compiled in 1973 by Geometrics, Inc. and released by the U.S. Geological Survey (1974). The aeromagnetic map was available at the onset of AMRAP field studies in Circle quadrangle. One of the authors (Weber) participated in the geologic mapping from 1978 through 1982. The geophysicist (Cady) made a preliminary interpretation of aeromagnetic data in 1979, and participated in geology mapping in 1979 and briefly in 1981, and conducted studies of the Circle Volcanics in 1981 through 1984. Helen L. Foster provided logistic support for geophysical studies in

1979 and 1981 and entertained many stimulating discussions on the use and significance of aeromagnetic and gravity data. Geologic hypotheses based upon aeromagnetic data have been tested in portions of the Circle quadrangle, especially in the southwest quadrant and in the east Crazy Mountains. Many hypotheses in the aeromagnetic interpretation, however, remain untested. In many cases the aeromagnetic interpretation and geologic map disagree.

The gravity map (Cady and Barnes, 1983) is based upon relatively sparse data. It helped to divide the quadrangle into areas of differing crustal density and (or) thickness, to identify a sediment-filled graben, to delineate areas of granitic plutons, and to identify a huge body of dense nonmagnetic rock--possibly dunite or gabbro. More closely spaced gravity data could help to delineate smaller features of geologic interest. In future AMRAP studies, these data could be efficiently collected during the geochemical sampling program.

A spectrally-colored rendition of the aeromagnetic map (figure 1) is easier to interpret than the contour map shown in plate 1, but the scale is inadequate for detailed studies. Therefore, the serious student of aeromagnetics in Circle quadrangle is advised to hand color a copy of plate 1.

Plate 2 is an interpretative map designed so the reader can identify magnetic anomalies and their geologic setting as they are discussed in the text. For simplicity, continuity of anomalies is somewhat exaggerated. The reader is referred to the magnetic contour map (plate 1) for the true configuration of anomalies.

REGIONAL GEOPHYSICAL TERRANES

Interpretation of the aeromagnetic and gravity maps suggests the subdivision of the quadrangle into three geophysical terranes. The southwestern three-fifths of the quadrangle coincides with the Yukon crystalline terrane of Churkin and others (1982) and also includes parts of other terranes in northwest Circle quadrangle (Foster and others, 1983); this region is characterized by a Bouguer gravity anomaly of -40 mgal or lower. It contains northeast- to east-northeast-trending magnetic highs and lows which are interpreted to reflect compositional variations in Paleozoic to Precambrian(?) metamorphic rocks and probable syntectonic granitic rocks.

Cutting across the quadrangle from east-southeast to west-northwest is an arcuate band of magnetic highs and a gravity gradient coincident with the Tintina fault zone. A broad magnetic high in the eastern Tintina fault zone is caused by a buried source about 4 km deep, which, because there is a weak gravity low accompanying the magnetic high, is inferred to be granitic. Further west, the Tintina fault zone contains shorter-wavelength magnetic highs and lows that may indicate exotic fragments caught up in the fault zone.

The area north of the Tintina fault zone is characterized by an east-west-trending belt of magnetic and gravity highs caused by known and inferred Paleozoic and early Mesozoic mafic and ultramafic rocks with oceanic affinities. The magnetic highs are linear or arcuate in the Crazy Mountains, where a coherent section of layered gabbros, some of which are strongly magnetic, occur in synclinal thrust remnants; magnetic highs are irregular or equant in the Yukon Flats, probably indicating buried mafic intrusive centers. A gravity low and area of low magnetic relief occur in the Yukon Flats along the western half of the northern quadrangle boundary. This region probably contains sedimentary rocks of unknown age.

METAMORPHIC TERRANE SOUTH OF THE TINTINA FAULT ZONE

Introduction

South of the Tintina fault zone, first-order variations in the magnetic field reflect the distribution of nonmagnetic granitic rocks and variably-magnetic metamorphic rocks. Lows GL1 through GL8 in the northwest and GL9 through GL13 in the southeast coincide with areas of mapped granitic rocks or suggest continuations of granitic rocks in the subsurface. Magnetic highs S1 through S13 are caused by polydeformed chloritic schist of the metamorphic terrane that we interpret to have been gently refolded around east-northeast-trending axes. Lows due to granite dominate the terrane northwest of highs S3, S5, and S8, and southeast of high S11. Magnetic high GH1 (T.8N, R.4E) is caused by a magnetic syenite pluton located in the Livengood B-1 and C-1 quadrangles. Uranium prospects are associated with the margins of this pluton in Livengood quadrangle. No magnetic plutons are found south of the Tintina fault zone in Circle quadrangle.

Lows Caused by Nonmagnetic Granite

All granitoids in Circle quadrangle, with the notable exception of the Victoria Mountain pluton, correlate with magnetic lows or featureless areas, and wherever measured, have magnetic susceptibility less than 0.1×10^{-3} emu/cm^3. This places them in the ilmenite series of Ishihara (1981). The non-magnetic granitoids in Circle quadrangle are biotite and biotite-muscovite granites, which Chappell and White (1974) call S-type granites and attribute to anatexis of sedimentary rocks. Hamilton (1984) questions the sedimentary source hypothesis, arguing that S-type granitoids crystallize from warm wet magma and I-type from hot dry magmas.

The nonmagnetic granites of Circle quadrangle, with the exception of the Hot Springs pluton, are elongate parallel to the strike of foliation, although they are unfoliated themselves. Some of them (e.g. GL9-10 below) clearly occur in the axes of antiforms defined by foliation dipping away from the center of the plutons. Contact metamorphism (shown on the geologic map of Foster and others, 1983) is rare compared to the well-defined contact metamorphic aureole surrounding the magnetic I-type Victoria Peak granodorite. We suggest that the nonmagnetic S-type granites of Circle quadrangle were intruded warm, not hot, and probably deep, so that there was no great temperature contrast with the surrounding metamorphic rocks and no pronounced contact aureole was formed. Hence, they may be anatectic granites. Intrusion must have followed the formation of D_1 axial plane schistisity (Cushing and Foster, 1982) because the granite is not foliated; but intrusion could have been as late as D_4 open folding that made the antiform in which the granite occurs. Early Tertiary K/Ar ages (Wilson and Shew, 1981) from the nonmagnetic granites probably do not date the intrusions, but rather date a late thermal event or uplift of a granite which has been held at depth at a temperative higher than the blocking temperature. (Hutchinson, 1983).

The Lime Peak biotite granite pluton lies near the center of magnetic low GL1 (T.9N, R.5E). The breadth of the magnetic low compared to the surface exposure of the pluton, and a coincident gravity low, suggest that the pluton has deep roots and may widen at depth.

Within low GL1, at the margins of the mapped pluton, are magnetic high M1 and low M2, which may indicate either mineral zonation within buried portions of the pluton or contact metamorphic aureoles. Stream sediment geochemistry (Tripp and others, 1983) shows anomalies parallel to the aeromagnetic anomalies. For example, high M1 coincides with a zone of anomalous fluorine, and low M2 with a zone of anomalous lanthanum. More detailed aeromagnetic data over the Lime Peak area might help to delineate mineral zonation within the pluton and surrounding rocks.

Magnetic low GL2 (T.8N, R.5E) marks a small nonmagnetic granite pluton that was discovered while looking for the cause of the magnetic low. The cause of high M3, which wraps around the west and north sides of the pluton, is interpreted to be a contact aureole.

Magnetic lows GL4 and GL5 coincide in many places with the Quartz Creek and Mt. Prindle granite plutons, but the magnetic lows cover a much larger area than the exposed plutons. Low GL6 coincides with hypabyssal felsic igneous rocks and a small pluton that suggest the presence of a larger pluton at depth. Magnetic low GL7 occurs in an area of exposed quartzite, but it lies along trend with the hypabyssal felsic intrusives. A broad gravity low, poorly-defined by available data, roughly coincides with magnetic lows GL3 through GL6. We conclude, therefore, that the area encompassed by these lows, and possibly low GL7 as well, is underlain by nonmagnetic granitic intrusions.

An unresolved problem is that the broad band of magnetic lows, of which GL6 is the lowest part, is not offset by a fault (informally known as the Pinnell Mountain fault) near Table Mountain (T.7N, R.9E). Neither does the fault offset anomalies S5, S6, or S9 where it crosses them further south. Cushing and others, (1982) suggest the fault has about 2 km of left slip offset. This amount of offset is easily accomodated by the aeromagnetic data. Weber emphasizes that felsic hypabyssal rocks showing on the geologic map on the northwest side of the fault in T.7-8N., R.9E reappear on the southeast side of the fault (although they are not shown on the geologic map) in T.9N, R.11E, indicating about 17 km of left-slip motion on the fault. Cady counters that the broad area of magnetic lows southeast of the fault could indicate abundant buried hypabyssal intrusives, rending correlation of specific hypabyssal intrusive bodies across the fault impossible. It is also possible that magnetic lows are not offset across the fault because the hypabyssal plutons are younger than the faulting.

Although Menzie and others (1983) refer to contact metamorphic rocks in their tracts II and III, which are roughly coincident with parts of magnetic lows GL3 and GL7, magnetic anomalies do not appear to be very useful in this area for locating contact metamorphism. Menzie (written commun., 1984) says that the scheelite-bearing tactite and skarn deposits in the area do not contain magnetite. Most of the magnetic highs in the area can best be explained by compositional variations in quartzite and schist. A possible exception, magnetic high M4? (T.7N, R.4-6E), has very low amplitude, and occurs in mapped quartzite over an inferred buried pluton. It may indicate a contact metamorphic aureole.

Several local high-amplitude magnetic lows, with local amplitudes of 50 to 120 nT, occur on the axes of lows GL4, GL5, and GL6. The large amplitude of these negative anomalies, isolated from any positive anomalies, suggests that they may be caused by reverse remanent magnetization. Ground magnetometer profiles made to test this hypothesis are shown in figure 2, profiles I and K (T.8N, R.6E and T.7N, R.7E on plate 2). Profile I, and to a lesser extent K, show narrow magnetic lows permissive of reversely magnetized rock at shallow depths, but no magnetic rock was found at the surface. All hypabyssal intrusive rocks tested had magnetic susceptibilities close to the lower limit of detectability (0.1×10^{-3} emu/cm^3) of our field susceptibility meter. Remanent magnetization of samples 21 and 22 is too low to cause the local lows. Hence it is uncertain whether lows GL4, GL5, and GL6 are caused partly by reverse remanent magnetization.

Magnetic lows GL8, GL7, and the eastern part of GL6 form a roughly circular pattern coincident with the high ground of Pinnell Mountain, Porcupine Dome, Eagle Summit, and Mastodon Dome. As high ground in Circle quadrangle characteristically occurs in areas of known and inferred granite, the lows may indicate a buried nonmagnetic pluton.

If mineralogical data are also considered, the arcuate pattern of magnetic highs and lows centered between Pinnell Mountain and Mastadon Dome is strongly suggestive of a buried pluton with possible economic importance. Nonmagnetic mineral concentrates of stream sediments (Tripp and Crim, 1983a) show mineral zonation congruent with the arcuate magnetic anomaly pattern. Stibnite occurs in the center, surrounded by arsenopyrite and galena. The area also contains the headwaters of most of the streams in the Circle placer gold mining district.

The continuity of magnetic lows (e.g., GL6) as well as inferred plutons and associated hypabyssal rocks across the Pinnell Mountain fault suggests a similar origin for gold placers (see Menzie and others, 1983, for location) in the western and central portions of Circle quadrangle.

GL9 and GL10, in the southeastern quadrant of Circle quadrangle, form an arcuate pattern of magnetic lows open to the southwest. The magnetic lows are associated with the broadest and highest-amplitude gravity low in the quadrangle. The magnetic lows are caused by known and inferred granitic plutons that wrap around a well-defined, southwest-plunging synform in the metamorphic rocks. The breadth and amplitude of the gravity low in southeastern Circle quadrangle suggest that the plutons there may coalesce at depth.

Magnetic low GL12 (T.7N, R.14-16E) is a reentrant in the flank of the large magnetic high GH3 caused by a buried magnetic pluton in the Tintina fault zone. When the magnetic data were high-pass filtered to suppress long-wavelength anomalies such as GH3, a short-wavelength magnetic low emerged coincident with the non-magnetic Circle Hot Springs pluton. Another irregularly shaped, magnetic low (in T.6N, R.18E) visible in the high-pass filtered data is labeled (GL13), the parentheses indicating that the low is not clearly visible on the unfiltered map because of interference from high GH3. It coincides with a mapped granitic pluton.

The Chena Hot Springs pluton (T.2-3N, R.5-10E) has no expression on the unfiltered aeromagnetic map (plate 1), and showed only as an area of somewhat subdued anomalies on the high-pass filtered map. Hence the Chena Hot Springs pluton probably has variable magnetic properties similar to those of the surrounding metamorphic rocks. Abundant xenoliths of schist and quartzite indicate that the pluton has been contaminated by country rocks. An alternate explanation for its lack of magnetic expression is that the pluton occurs as a thin thrust plate, and the magnetic variations are caused by underlying metamorphic rocks. A magnetic gradient 3 km west of Chena Hot Springs (T.3N, R.8E) indicates that magnetic rock is buried about 1700 m beneath the exposed granite surface.

Highs Caused By Magnetic Schist

The most perplexing problem in interpreting the aeromagnetic map of Circle quadrangle has been to explain the magnetic highs over the Yukon crystalline terrane. The problem is twofold: 1) In the majority of cases, despite careful surface checking with a magnetometer (fig. 2) and a portable susceptibility meter under the axes of magnetic highs, magnetic rocks could not be found; 2) magnetic anomaly trends commonly cross from one geologic map unit to another. This occurrs for most of the east-northeast-trending anomalies S1 through S13, which follow the structural grain, as well as for anomalies S14 through S24, which trend north-south or otherwise contrary to structural grain.

An explanation that addresses both the preceding problems is that the surface geology is separated from the sources of the anomalies by shallow subhorizontal thrusts (H. L. Foster, oral commun., 1983). Depth estimates to the magnetic sources indicate that this explanation is unlikely. Maximum depth in meters to magnetic sources, calculated by measuring the widths of steepest magnetic gradients (a simplified variation of the method of Vacquier and others, 1951) and subtracting the flight height of the aircraft are plotted on the aeromagnetic interpretation map, plate 2. The maximum depth to source of the magnetic highs labeled "S" ranges from 0 m to 1700 m below the surface. Depths as shallow as 300 m are common in the Yukon crystalline terrane. The magnetic highs occur over a wide range in elevation, but many of them occur on ridges standing 500 m or more above adjacent valleys. If there were subhorizontal thrusts 300 m below the ridge tops, then the underlying, magnetic rocks of the lower thrust plate should be exposed in the valleys. This possibility cannot be excluded, for figure 2 of Foster and others (1983) shows that nearly all foot traverses and the majority of spot observations were made on ridges. Sufficient observations were made in valleys, however, to show that dominant rock types in the valleys are not radically different from rock types on the ridges. In the following paragraphs, we shall develop an alternative explanation based upon the hypothesis that if easily-eroded, magnetic schist, and more resistant, nonmagnetic quartzite occur in layers, observations made on the ridges will selectively sample the resistant quartzite.

Magnetic high S6 is the only magnetic high south of the Tintina fault zone along which magnetic rock could consistently be found. Sample sites 1 through 10 all contain variants of quartz-muscovite-chlorite-magnetite schist. The mean magnetic susceptibility of chlorite-bearing pelitic schists at sites where magnetic rock was found is $1.2 \times 10^{-3} \pm 1.1 \times 10^{-3}$ emu/cm^3.

Calculations show that rocks with this susceptibility can cause anomalies with the observed amplitude of 100 to 150 nT if they occur at or close to the surface over a cross-strike width of 2 km and have a thickness of 2 to 3 km. An example of such an anomaly source is shown in figure 3.

If the rocks contain remanent magnetization, the source could be thinned proportionately. Remanent magnetization was not measured. Surface magnetometer profiles, however, can be used to determine whether the magnetic source is deep or shallow. If the source is shallow, local variations in the magnetic field establish the maximum variation in total magnetization (remanent plus induced) occurring near the surface. Surface profiles A and H (fig. 2) (T.4N, R.5E and T.5N, R.8E) across anomaly S6 show short wavelength anomalies with maximum amplitudes of only 200 to 300 nT. This is only twice the amplitude of the aeromagnetic high--indicating that local variations in the total magnetization, including remanent plus induced, cannot be more than about twice the mean magnetization of the source of the aeromagnetic high determined by modeling. Hence remanent magnetization can at most double the mean magnetization of the aeromagnetic source, which must therefore have a thickness of at least 1 to 1.5 km. Because the source rocks are very inhomogeneous, so the maximum magnetization estimated from a surface magnetometer traverse is unlikely to be present throughout a large body, the thickness of 2 to 3 km modeled using susceptibility alone is probably a better estimate.

A second conclusion from the magnetic modeling is that the depths estimated by the Vacquier method are deeper than those obtained by magnetic modeling using reasonable values of susceptibility. Modeling required the source to be at the surface where profile A-A′ crosses anomalies S5 and S6, whereas maximum depths estimated by the Vacquier method were 490 and 300 m respectively. Extrapolating to the rest of the quadrangle, we conclude that most of the sources shown at depths of 300 to 500 m by the Vacquier method should outcrop at the bedrock surface.

We are left, therefore, with an enigma. Magnetic interpretations and modeling require that there be a great volume of magnetic rock in the shallow subsurface, but magnetic rocks rarely crop out. Cady and Hummel (1976) encountered a similar problem near Nome in the Seward Peninsula, but the results were inconclusive because they did not have a portable susceptibility meter. They hypothesized that oxidation due to weathering had destroyed magnetite near the surface, because magnetic anomalies in the Nome area commonly coincide with swales. In Circle quadrangle the role of weathering in oxidizing magnetite is unknown. A map was made showing the distribution of thin sections containing opaque minerals. Opaque minerals occur indiscriminately in both magnetic highs and lows.

Inferred surface contacts of the magnetic schist were drawn beneath the steepest gradient zones of anomaly S6. The contacts were deflected towards the steep gradient side of assymetrical highs, on the premise that magnetic sources dip away from steeper gradients. The inferred outcrop pattern is narrower, but more continuous along strike, than the magnetic schist unit mapped by Foster and others (1983).

An inferred magnetic outcrop boundary was drawn around anomaly S5 as well, even though no magnetic rocks were found in the field, because outcrop is required by the magnetic model. A surface magnetometer traverse (profile C, fig. 2, T.5N, R.6E) shows that magnetic rocks occur within 100 m of the surface. Another ground magnetometer profile (G, T.4N, R.5E) shows that at that location, the source is probably buried.

The configuration of highs S5 and S6, separated by a deep magnetic low L1, is suggestive of an antiformal source mass containing a breached magnetic layer. The field drops abruptly southeast of high S5, but rolls off gently through the undulations of highs S4 and S3, to the northwest. This pattern suggests a magnetic source with a regional dip to the northwest. A similar analysis shows that the source of S6 dips to the southeast.

Magnetic profile A-A′ (fig. 3) was modeled using a nonlinear inversion technique (M. W. Webring, written commun., 1983). For a wide range of starting models, iterative modeling tended to converge on sources that looked like antiforms. Three examples of final models are shown in figure 3. All have bottoms that are bowed up under low L1. Models A and B agree with the observed topography - Smith Creek has a valley 100-200 m deep along the axis of the magnetic low. The uppermost magnetic layers in the antiform are breached, but the main cause of low L1 is the subsurface bulge of nonmagnetic rock, either quartzite or granite. Model C fits the observed magnetic field better than models A and B, but it is geologically less plausible. There is no geologic explanation for the 500 m valley shown in the top of the magnetic layer, unless deep weathering is localized in the axis of the antiform. Magnetic chlorite-bearing pelitic schist, with a susceptibility of about $1x10^{-3}$ emu/cm^3, dips off in an undulating fashion to the southeast and northwest. It cannot be determined from the magnetic data whether the magnetic schist dips beneath the Mt. Prindle pluton to the northwest, truncates against the pluton at depth, or crops out in the vicinity of high S3.

Other magnetic highs of the "S" series are not so well defined as S5 and S6. Amplitudes are lower, and calculated depths are often greater, especially in the southeast. Magnetic rocks could generally not be found. An explanation for these broader anomalies is that magnetic schist approaches, but does not reach, the surface in the axes of antiforms under magnetic highs. Although this explanation smacks of special pleading, it is justified in the following paragraph. In this scheme synforms cause magnetic lows. Axes of magnetic highs and lows that fit the scheme are labeled with antiform and synform labels on plate 2. Highs and lows that do not fit the scheme have axes labeled by ball and bar symbols only.

Magnetic highs labeled "S" require the presence at the surface or in the shallow sursurface of one or more layers of magnetic rocks with susceptibility of at least $1x10^{-3}$ emu/cm^3, or equivalent remanent magnetization, and a thickness of 1 km or more. Abundant magnetic source rocks were found only under high S6. Hence we propose a model in which magnetic chloritic pelitic schist, occurring in one or more layers with quartzite and, in the east, nonmagnetic schist, has been gently folded about east-northeast trending axes. Many of the magnetic highs are inferred to occur at the crest of antiforms that bring magnetic schist close to the surface. Quartzite forms a resistant carapace covering the less resistant schist, making it difficult to observe the schist, especially on the ridges where most of the geologic traverses have been made. Only where the antiforms have been breached, as along S6, are exposures of magnetic schist abundant.

Nonmagnetic granites indicated by magnetic lows GL1 through GL9 occur in trends parallel to the magnetic highs attributed to schist. We interpret these granites as the cores of east-northeast trending antiforms developed during a late open-folding event (Cushing and Foster, 1982) that refolded preexisting recumbent folds and metamorphic foliation. Magnetic highs such as S3, S11, and S18 occur on the limbs of granite-cored antiforms. Magnetic schist should be exposed under these highs, according to the model, because they occur on the breached flanks of antiforms. However, no magnetic rocks were found under anomalies S3 and S18. Magnetic amphibolite and serpentinized ultramafic rock were found under high S11.

Other magnetic highs, such as S1, S2?, S3?, and S12 occur between major granite plutons, in places where gravity lows indicate granite at depth. These highs are interpreted to be caused by synformal roof pendants of chloritic schist, but magnetic rocks were not found.

The model is undoubtedly simpler than the real situation in Circle quadrangle. Although quartzite, nonmagnetic pelitic schist, and magnetic chlorite-bearing pelitic schist reflect original compositional layering in the protolith, isoclinal folding at several scales (Cushing and Foster, 1982) has disrupted continuous layers and repeated single layers. The synforms and antiforms of plate 2 have been drawn as if there were a single magnetic layer. The simple model provides a unifying hypothesis that can be tested and modified by further geologic mapping.

Magnetic high S1 crosses the boundary between the Beaver and Yukon crystalline terranes of Churkin and others (1982), suggesting that the boundary is incorrect in detail. On the geologic base of plate 2, the boundary separates grit, quartzite, and argillite (PzpЄgq) of the Beaver terrane from quartzite and quartzitic schists (PzpЄq) of the Yukon Crystalline terrane. Magnetic highs commonly occur in the latter unit, but not in the former. A minor adjustment of the boundary to north of high S1 in T.9N, R.6-7E would satisfy the magnetic data. The adjustment is permissible on geologic grounds because the rock type is queried in the northwest corner of T.9N, R.6E.

Highs Caused by Metamorphosed Ultramafic Rocks

Within three of the magnetic highs labeled "S", magnetic metamorphosed ultramafic rocks were found. High U1 (T.3-4N, R.4-5E), identified as the continuation of high S7, has a higher amplitude (232 nT higher than a nearby low) than other highs labeled "S" and is almost certainly caused by the ultramafic rocks. At U2 (T.5N, R.15E) magnetic amphibolite and serpentinite were found. The relatively low amplitude of the aeromagnetic high (53 nT) may be because the magnetic rocks occur in a thin thrust plate (Foster and others, 1983). High S11, within which the magnetic ultramafic rocks occur, does not coincide with the mapped continuation of the thrust plate. Hence, the occurrence of ultramafic rock in S11 may be coincidental.

A belt of serpentinized peridotite was mapped by Foster and others (1983) in magnetic high U3 (T.6N, R.17-18E). Magnetic high U3 is superimposed on high GM3 and better defined on a high-pass filtered version of the aeromagnetic map (not shown).

Both magnetic chloritic pelitic schist and metamorphosed ultramafic rocks are found in east-northeast trending magnetic highs in the Yukon crystalline terrane. The simplest explanation is that the two rock types are infolded. However, two of the ultramafic occurrences coincide with mapped thrust plates of limited regional extent suggesting that the schist and ultramafic rocks are unrelated. In future mapping in Circle quadrangle, magnetic studies could play an important role in working out the relationships between thrust plates.

Highs U4 and U5 are is discussed in connection with the Tintina fault zone.

TINTINA FAULT ZONE

Physiographically, the Tintina fault zone begins north of the resistant metamorphic rocks of the Yukon crystalline terrane. In the eastern third of the map area, these resistant rocks crop out as far north as the 1000 ft contour, almost at the crest of a large anomaly in the flats, labeled GH3, that we call the Medicine Lake magnetic high. The source of the Medicine Lake high is nowhere exposed. The steepest gradient zones bounding the high are about 7 km wide, indicating a maximum depth to source of about 7 km, but magnetic modelling discussed below indicates the depth to the top is about 4 km. The Hot Springs fault, which bounds the Yukon crystalline terrane, must either dip to the southeast to accomodate the inferred magnetic pluton that broadens with depth, or the pluton has intruded the fault zone.

A broadly irregular magnetic high extends west-northwest along the Tintina fault zone from the Medicine Lake magnetic high. The source of this subdued magnetic high is not known. Lack of coherence within the high suggests that a once-continuous source may have been disrupted by faulting.

An intense magnetic high over Victoria Mountain (T11N, R. 4 E.) is caused by hornblende-biotite granite with a mean susceptibility of $1x10^{-3}$ emu/cm^3 and a density of about 2.63 g/cm^3--approximately the physical properties required to model magnetic and gravity profiles over the Medicine Lake magnetic high. Biotite and hornblende occuring together indicate that the Victoria Mountain pluton is I-type granitoid (Chappell and White, 1974). Its high magnetic susceptibility makes it a magnetic series granitoid (Ishihara, 1981). It has a pronounced contact metamorphic aureole, suggesting that it intruded hot into cooler rocks in the upper crust.

Three magnetic highs associated with ultramafic rocks occur in close association with the Tintina fault zone. High U3 (T. 6N, R.17-18 E) is caused by serpentinized peridotite occurring 1 to 4 km south of the Tintina fault zone. According to Foster and others (1983), it is infolded with mafic and pelitic schists of the Yukon crystalline terrane and is probably not related to the Tintina fault zone. High U5 (T.12N, R.5-6E) connects two outcrops of serpentinized peridotite that Foster and others assign to the northwestern Circle quadrangle area. The magnetic anomaly shows that the serpentinized rock is continuous between the outcrops. We interpret high U5 as the probable northern boundary of the Tintina fault zone because the faulted serpentinite is alined with the magnetic gradient along the Preacher Creek fault.

High U4 (T.10N, R.9E) is caused by a body of metamorphosed ultramafic rocks that contain up to 50% magnetite (samples 33 and 34, table 1).

Protolith has been variously identified as gabbro, pyroxenite, or peridotite. It is a very uncommon rock. Sample 34 contains tectonic fragments of fine-grained calcareous sandstone similar to calcareous siltstone and sandstone found in close association with cumulus peridotite north of the Tintina fault zone in the East Crazy Mountains and along the Yukon River south of Circle City. High U4 and high G7 (caused by peridotite and layered gabbro) in the East Crazy Mountains can be connected by a curved line labeled X-X′. The line has a possible extension X′-X′′ that links the East Crazy Mountains to magnetic high G8. It is possible that the magnetic sources G1?, U4, and G3? have been thrust south across the Tintina fault zone and onto the Yukon crystalline terrane, but this is very speculative. The nature and origin of the very magnetic rocks that cause high U4 is not understood.

Nonmagnetic gabbro was found at the surface at G2 (T.10N, R.9E). Bedrock was not located under high G3. High G1? has not been visited. All three of these magnetic highs are tentatively interpreted to be caused by magnetic gabbro displaced by thrusting from the terrane north of the Tintina fault zone. Alternatively, Weber suggests that highs G1?, G2, G3? and possibly U4 may be caused by gabbro and serpentinized ultramafic rocks within the argillite, grit, and quartzite unit (Pz€ta) of Foster and others (1983).

Magnetic high M5 wraps around low L9 in the geologically unique region around VABM Vrain (T.11N, R.6-7E) (discussed by Foster and others, 1983). The arcuate high appears to be truncated in the south by the Hot Springs Fault. Magnetic rock was not located. The magnetic source is covered by alluvium and nonmagnetic argillite, felsic tuff, quartzite, and conglomerate (MzPzat). Low L9 coincides approximately with an area containing tuffaceous rocks. We infer that there is a genetic relationship between low L9 and high M5. We speculate that L9 is caused by a buried pluton or swarm of felsic dikes, and M5 is caused by a contact metamorphic aureole or ring dike. Tuff surrounded by an arcuate structure is suggestive of a caldera. Barium, zinc, and nickel anomalies coincide with the western part of the ring structure (Tripp and Crim, 1983b).

Magnetically, the Victoria Mountain pluton, the partial ring structure around VABM Vrain, and the serpentenite associated with high U5 seem to belong to the Tintina fault zone. Therefore, we have extended the Tintina fault zone to the west border of Circle quadrangle on plate 2.

OCEANIC TERRANE NORTH OF THE TINTINA FAULT ZONE

Magnetic highs G5 through G8 are caused by layered gabbros and cumulus peridotite belonging to the Circle Volcanics, which are correlative with the Rampart Group of Mertie (1937). Highs G5 through G8 are part of a nearly continuous trend of magnetic highs caused by gabbros and cumulus peridotite of the Circle Volcanics and Rampart Group that extend from the Yukon River in eastern Circle quadrangle across the northern part of Circle quadrangle and west-southwest across Livengood and Tanana quadrangles. The trend of magnetic highs coincides with a related trend of gravity highs. Together, these geophysical anomalies mark the southern, leading edge of a terrane (called the Tozitna terrane by Jones, 1983) that we interpret to be thrust southward over lower density crust of the Yukon-Tanana upland.

Lows L10 and L11 are caused by nonmagnetic sedimentary rocks in the southern parts of the East and West Crazy Mountains and the area around Victoria Creek (T.12N, R.4-5E). The magnetic lows are nearly continuous across the width of the quadrangle, forming a boundary between magnetic highs over the Circle Volcanics and highs associated with the Tintina fault zone.

The best outcrops of Circle Volcanics occur along the east bank of the Yukon River (T.9-10N, R.18E). Aeromagnetic anomalies are truncated by the eastern map boundary, however, and exposures are tree-covered away from the river. A detailed study of the section along the Yukon River is underway. Units identified along the Yukon can be mapped in the East Crazy Mountains, where the aeromagnetic map and relatively bare hillsides allow units to be traced along strike.

The northern part of the Yukon River section (T.10-11N, R.18E) is more than 5 km thick, although it is possible that some of this thickness represents repetition by faulting. Within the section are layered gabbro sills up to several hundred meters thick intruding chert, argillite, and distal turbidite mudstone; noncumulus gabbro; and basalt flows with indistinct pillows. Further south (T.9N, R.18E) a 4-km thick section was measured that contains gabbro and diabase sills intruding chert, argillite, and calcareous quartz-rich siltstone and basalt. Cady (1983) proposed a laccolith model in which the intrusive rocks of the Rampart Group intruded oceanic sediments in an oceanic plateau or primitive magmatic arc.

Most of the gabbro section is weakly magnetic ($k = 0.02 - 0.12 \times 10^{-3}$ emu/cm^3 measured with a susceptibility meter more sensitive than that used for most of the field work). Rare noncumulus gabbro was magnetic ($k = 1.0 \times 10^{-3}$ emu/cm^3). Several layers, usually occuring in close proximity to each other in the layered gabbro section, are very magnetic and form valuable marker horizons in the East Crazy Mountains. The magnetic layers are sheared, serpentinized wehrlite ($k = 2 - 10 \times 10^{-3}$ emu/cm^3); gabbronorite ($2 - 7 \times 10^{-3}$ emu/cm^3); dark grey tonalite or quartz diorite ($2 - 10 \times 10^{-3}$ emu/cm^3); and very tough, hard, very coarse grained wehrlite with a knobby weathering surface ($k = 0.8 - 2.5 \times 10^{-3}$ emu/cm^3).

A magnetometer profile was made along the Yukon River from a boat (figure 2R). Two magnetic peridotite layers are apparently truncated at the river by a fault, because magnetic highs were not observed along strike in the river. The isolated magnetic highs occurring at the Yukon River (T.9-10N, R.18E) are interpreted to be caused by a klippe of Circle Volcanics thrust south over nonmagnetic rocks. Other isolated magnetic highs probably carried by buried klippen of Circle Volcanics occur in the north flank of high GH3 in T.9-10N, R.14-16E.

The best mappable exposures of Circle Volcanics occur in the East Crazy Mountains under magnetic highs G6 and G7 (T.11N, R.11-13E). The magnetic highs are an island within the magnetic low (L10 and L11) north of the Tintina fault zone. Magnetic high G6 has steep gradients on the north, indicating that magnetic rock dips south. Magnetic high G7 has steep dips on the south, indicating that magnetic rock dips north. Together the anomalies delineate a synform of magnetic rock. Geologic mapping using aeromagnetic maps as a guide confirmed that highs G6 and G7 are underlain by a syncline of layered gabbro intruding marine sedimentary rocks. Within the section are two or three layers of highly magnetic rocks, either gabbronorite or cumulus wehrlite, like those studies along the Yukon River. The magnetic layers are distinctive marker beds that are useful for geologic mapping. These magnetic layers, both mapped and inferred from magnetic interpretation, are labeled "m" on plate 2.

South-southeast of the syncline delineated by magnetic highs G6 and G7 is a triangular region of nonmagnetic diabase, fine grained gabbro, and chert. This region, which widens eastward from a point in T.11N, R.12E to 3 km in T.11N, R.13E, is not differentiated from the magnetic rocks of the syncline on the map of Foster and others (1983). We have observed, however, a probable fault-line scarp separating the syncline containing magnetic rocks from the triangular exposure of nonmagnetic rocks in T.11N, R.12E. On this basis, because of the abrupt change in lithology indicated by the aeromagnetic map, and because the magnetic high G6 and G7 are a magnetic island surrounded by lows, we have drawn a thrust fault around the syncline. We interpret the syncline as an erosional remnant of a thrust plate that was once connected with magnetic rocks further north, possibly those that cause highs G5 and G8.

Radiolaria of Late Triassic age (Map number 24 and 27 and Table 2 of Foster and others, 1983) have been identified in cherts from the nonmagnetic triangle. Radiolaria were collected in the syncline containing magnetic rocks, but a date has not yet been obtained.

Subdued magnetic highs labeled V1 are caused by magnetic diabase in the Little Crazy Mountains. A 30 mgal gravity high centered on the Little Crazy Mountains has limbs that correlate with magnetic highs G5 through G8, but the crest and northeastern flank of the gravity high coincides with magnetic low L12. The gravity data are consistent with the presence of low-density sedimentary rocks beneath the eastern part of magnetic low L12; but the gravity high over the western part of L12 indicates the presence of a deep, massive, nonmagnetic or weakly-magnetic body. Possible candidates are dunite, which is nonmagnetic when unserpentinized, or nonmagnetic gabbro. Neither explanation is very satisfying, for unserpentinized dunite is rare in the Earth's crust, and large bodies of nonmagnetic gabbro are unknown in the Rampart Group.

Ovoid or irregular magnetic highs labeled V2 occur in the Yukon Flats north and west of the Little Crazy Mountains. Steep gradients indicate shallow sources. The magnetic highs seem to be unrelated to the much broader gravity high in the Little Crazy Mountains. We tentatively infer that highs V2 are caused by mafic plugs or dikes associated with volcanic centers that have been eroded away and covered by fluvial deposits and loess.

Anomalous antimony, thorium, and zinc occur north of the Tintina fault zone, entirely within the oceanic terrane and between 15 and 35 km north of the buried Medicine Lake pluton (Tripp and Crim, 1983a, b; Tripp and others, 1983). The anomalies were found in stream sediment concentrates from northeast-flowing streams that drain the sedimentary portion of the east Crazy Mountains. The mineralogical and geochemical anomalies cross the trend of magnetic high G8 and occur within a major gravity high - hence it is unlikely that they are caused by a nearby hidden felsic pluton. We suggest that the anomalous stream sediments were washed into the oceanic terrane from a southern source within or south of the Tintina fault zone.

REGIONAL GRAVITY AND MAGNETIC MODEL

Figure 4 is a gravity and magnetic model calculated along profile B-B′ to determine crustal structure across the Tintina fault zone in the center of the buried Medicine Lake pluton. No seismic refraction data are available to constrain the model, so structures shown deeper than 10 km are purely hypothetical.

Both the gravity and magnetic fields are low in the south over a major pluton of S-type granite. The gravity field rises over the schist terrane to the north; the magnetic field shows short wavelength anomalies (not modeled) caused by east-northeast trending units of magnetic schist and infolded ultramafic rocks.

The broad Medicine Lake magnetic high and a narrow gravity low coincide over the Tintina fault zone . The magnetic high is caused by an inferred buried pluton of I-type granite. The pluton is shown as a broad, flat, body at the shallowest depth that will reproduce the observed gradients of the magnetic high. Alternatively, the pluton could be somewhat deeper and narrower. The gravity low is too narrow to be caused by the magnetic pluton. It is shown in the model to be caused by a small sedimentary basin beneath Medicine Lake.

The occurrence of the narrow gravity low precisely in the axis of the Medicine Lake magnetic high is probably not a coincidence. A possible explanation is that overlying rocks have been stoped into the pluton, causing a graben to form centered on Medicine Lake. The north boundary of the graben is a normal fault marked by a 6-13 m scarp in Quaternary deposits. Regionally, the Medicine Lake magnetic high coincides with an area of drainages that converge on the lowland surrounding Medicine Lake, suggesting subsidence associated with the source of the anomaly. Recent tectonic activity is confirmed by earthquake epicenters concentrated along the Tintina fault zone (L. D. Gedney, written commun., 1981), although the highest concentration of epicenters occur west of lat 145^{o}, outside the area of the Medicine Lake magnetic anomaly. The Circle Hot Springs, which occur on the south flank of the Medicine Lake magnetic high, could indicate that the pluton at depth is still cooling.

North of the Tintina fault zone, the Bouguer anomaly rises to about -20 mGal. In the isostatically-balanced model, most of the change in mean Bouguer anomaly between the Yukon crystalline terrane and the oceanic terrane is explained by a 2-km thinning of the crust to the north across the Tintina fault zone. Bodies of gabbro with density 2.89 g/cm^3 explain shorter wavelength gravity highs superimposed on the regional high of the oceanic terrane.

Alternatively, the lower crust of the oceanic terrane could be thicker or have a lower density, permitting thicker high-density bodies in the upper crust. Hence, the configuration of dense, magnetic gabbro bodies in the oceanic terrane is uncertain.

For simplicity, we required both gabbro bodies to have the same density and susceptibility. A least-squares routine determined susceptibility for both bodies to be very low - 0.2 x 10^{-3} emu/cm^3 - probably because the magnetic high caused by the buried Medicine Lake pluton interfered with the high between km 15 and km 20. A higher susceptibility (0.5×10^{-3} emu/cm^3) in the gabbro body at km 35 would help to make the calculated anomaly match the observed.

CONCLUSIONS

Three terranes are delineated by magnetic and gravity data. The metamorphic terrane south of the Tintina fault has low gravity overall and local lows over exposed and inferred granite plutons. Magnetic lows occur over S-type granites occurring in the cores of antiforms. Magnetic highs are caused by chlorite-bearing pelitic schists and metamorphosed ultramafic rocks occurring generally in east-northeast trending folds.

The Tintina fault zone is dominated by a broad magnetic high caused by the inferred Medicine Lake pluton, an I-type granite at least 4 km deep. Other magnetic highs within the zone are the highs caused by the Victoria Peak biotite hornblende pluton and a curious ring-shaped high.

North of the Tintina Fault is an oceanic terrane characterized by high gravity. Elongate east-west trending magnetic highs are caused by thrust plates of layered gabbro and peridotite thrust south from Yukon Flats. An isolated magnetic high in the East Crazy Mountains is caused by a synformal, allochthonous remnant of layered gabbro and peridotite occurring as laccoliths intruding marine sediments. Buried volcanic centers are the inferred cause of ovoid and irregular magnetic highs. A broad, 30 mGal gravity high centered over the Little Crazy Mountains has no associated broad magnetic high. Nonmagnetic dunite or gabbro may cause the gravity anomaly.

Several magnetic anomalies have implications for exploration. A magnetic high centered west of the quadrangle boundary is caused by a magnetic syenite. Uranium prospects are associated with this syenite in Livengood quadrangle.

The magnetic map suggests the presence of zonation within and (or) contact aureoles around portions of the Lime Peak pluton. Geochemical anomalies correlate with details of the magnetic anomaly. A detailed aeromagnetic map would be useful for mineral exploration of the Lime Peak pluton.

Broad magnetic lows indicate that felsic hypabyssal rocks northeast of Mt. Prindle are underlain by a large, nonmagnetic granitic pluton. Arcuate patterns of subdued magnetic highs and lows centered between Pinnell Mountain and Mastodon Dome correlate with zonation in stream sediment mineral concentrate data, and indicate a buried pluton with economic importance. Continuity of magnetic lows over known and inferred plutons between Mastodon Dome (the headwaters of the Circle placer gold mining district) and the Mt. Prindle region suggests a similar origin for gold placers in western and central portions of Circle quadrangle.

The curious ring-shaped magnetic high in the Tintina fault zone has felsic tuff in the magnetic low that forms its core. Barium, zinc, and nickel anomalies may be associated with a mineralized caldera, metamorphic aureole, or ring dike, the surface expressions of a shallow buried pluton.

Stream sediment anomalies of antimony, zinc, and thorium occur in the oceanic terrane in the northeastern part of the quadrangle. There is no magnetic evidence of a local felsic pluton, the expected source of the anomalies. Hence we infer that the anomalous sediments were carried into the oceanic terrane by fluvial processes, from a source within or south of the Tintina fault.

In the absence of seismic refraction data, no unique model for crustal structure can be determined by gravity modeling. From observation of gabbroic laccoliths in the east Crazy Mountains and along the Yukon River south of Circle City, we infer that the oceanic terrane contains thick crust of intermediate density.

REFERENCES CITED

Cady, J. W., 1983, Oceanic terranes of interior and western Alaska--Evidence for thick crust of intermediate density: in Howell, D. G., Jones, D. L., Cox, Allan, and Nur, Amos, Proceedings of the Circum-Pacific terrane conference, Stanford University Publications in the Geological Sciences, v. 18, p. 41-43, 1984.

Cady, J. W., and Barnes, D. F., 1983, Complete Bouguer gravity map of the Circle quadrangle Alaska: U.S. Geological Survey Open-File Report 83-170-D.

Cady, J. W., and Hummel, C. L., 1976, Magnetic studies of selected geologic and aeromagnetic features in southwest Seward Peninsula, west-central Alaska: U.S. Geological Survey Open-File Report 76-425, 56 p., 1 pl.

Chappell, B. W., and White, A.J.R., 1974, Two contrasting granite types: Pacific Geology, no. 8, p. 173-174.

Churkin, Michael, Jr., Foster, H. L., Chapman, R. M., and Weber, F. R., 1982, Terranes and suture zones in east central Alaska: Journal of Geophysical Research, v. 87, no. 135, p. 3718-3730.

Cushing, G. W., and Foster, H. L., 1982, Recumbent folding in the northeastern Yukon-Tanana upland, Alaska: Geological Society of America, Abstracts with programs, v. 14, no. 3, p. 158.

Cushing, G. W., Foster, H. L., Laird, Jo, and Burack, A. C., 1982, Description and preliminary interpretation of folds and faults in a small area in the Circle B-4 and B-5 quadrangles, Alaska: U.S. Geological Survey Circular 844, p. 56-58.

Foster, H. L., Laird, Jo, Keith, T.E.C., Cushing, Grant, and Menzie, W. D., 1983, Preliminary geologic map of the Circle quadrangle, Alaska: U.S. Geological Survey Open-File Report 83-170-A.

Hamilton, Warren, 1984, Review of Circum-Pacific plutonic terranes, J. A. Roddick, ed.: Episodes, v. 7, no. 2, p. 48.

Ishihara, Shunso, 1981, The granitoid series and mineralization: Economic Geology, 75th Anniversary Volume, 1981, pp. 458-454.

Jones, D. L., 1983, Tectonostratigraphic terranes of western North America--an overview: Geological Society of America, abstracts with programs, v. 15, no. 5, p. 384.

Menzie, W. D., Foster, H. L., Tripp, R. B., and Yiend, W. E., 1983, Map showing mineral resources of the Circle quadrangle, Alaska: U.S. Geological Survey Open-File Report 83-170-B.

Mertie, J. B., Jr., 1937, The Yukon-Tanana region, Alaska: U.S. Geological Survey Bulletin 872, 276 p.

Tripp, R. B., and Crim, W. D., 1983a, Mineralogical maps showing selected minerals in the nonmagnetic fractions of mineral concentrates of stream sediments, Circle quadrangle, Alaska: U.S. Geological Survey Open-File Report 83-170-F.

Trip, R. B., and Crim, W. D., 1983b, Maps showing geochemistry of stream sediment samples, Circle quadrangle, Alaska: U.S. Geological Survey Open-File Report 83-170-H.

Tripp, R. B., O'Leary, R. M., and Rizolli, D. A., 1983, Geochemistry of concentrates of stream sediments, Circle quadrangle, Alaska: U.S. Geological Survey Open-File Report 83-170-G.

Vacquier, V., Steenland, N. C., Henderson, R. G., and Zietz, Isidore, 1951, Interpretation of aeromagnetic maps: Geological Society of America Memoir 47, 151 p.

Wilson, F. H., and Shew, Nora, 1981, Maps and tables showing preliminary results of potassium argon age studies in the Circle quadrangle, Alaska, with a compilation of previous dating work: U.S. Geological Survey Open-File Report 81-889.

U.S. Geological Survey, 1974, Aeromagnetic map of the Circle quadrangle, northeastern Alaska: U.S. Geological Survey Open-File Report 74-1101.

Figure 1. Spectrally-colored aeromagnetic map of Circle quadrangle, with complete Bouguer gravity anomaly contours overprinted in black.

Figure 2A-2R. Ground magnetometer profiles. For location see plate 2. Only a few of the 18 profiles are discussed in text. The rest are provided as basic reference data.

Figure 3. Magnetic models along profile A-A′. Outlines of the different magnetic rocks shown by symbols that correspond to calculated anomaly curves. Magnetic susceptibility of each model = 1×10^{-3} emu/cm^3. All three source bodies are antiformal. Vertical exaggeration 2:1.

Figure 4. Cross-section of two-dimensional gravity and magnetic model along profile B-B′ (plate 2). Regional field of 40 nT removed from observed magnetic data. Density in g/cm^3. Susceptibility k in units of 10^{-3} emu/cm^3. Some labels omitted to save space: e.g., the mafic schist body has a density of 2.71 g/cm^3 and a susceptibility of 0.2×10^{-3} emu/cm^3. Bodies with no susceptibility shown are assumed to be nonmagnetic.

Table 1.--Magnetic properties and mineralogy of selected samples

Map Number[1]	Quad	Twp.	Rng.	Field No.	Magnetic Susceptibility[2]	Remanent Magnetization[3]	Rock Name[4]	Thin section mineralogy or Field rock name[5]
1	A6	4N	5E	79AJC2D	0.0-0.5-2.2		pelitic schist	qtz+wh mica+chl+plg+gar+opaq
2	A6	4N	5E	79AFr106A	0.2-1.0-3.5		pelitic schist	wh mica+plg+chl+qtz+opaq+gar
3	A6	4N	5E	79AWr50	0.1-1.0		pelitic schist	wh mica+qtz+chl+plg+gar+opaq+bio
4	A6	4N	5E	79AWr53	0.4-1.2-2.3			"greenschist"
5	A6	4N	5E	79AWr54	0.3-0.5			"garnetiferous chl qtz musc. schist"
6	A6	4N	6E	79AWr61	1.4-2.3			"qtz chl musc schist"
7	B5	5N	8E	79AFr6015	2.4-3.0		felsic schist	qtz+plg+chl+opaq+bio+gar+epi
8	B5	5N	8E	79AJC13D	0.4-3.0		quartzite	qtz+plg+chl+wh mica+opaq
8	B5	5N	8E	79AJC14	0.4-0.7		pelitic schist	qtz+wh mica+chl+plg+opaq
9	B5	5N	8E	79AWr117	visible magnetite			"chloritic schist"
10	B5	5N	8E	79AWr133A	0.5-0.6			"schistose mgt chl musc quartzite"
11	A2	5N	15E	79AJC50A,B	0.1-2.6		schist or amphibolite	plg+amp+chl+qtz+epi+opaq
12	A2	5N	15E	79AFr236	0.1-1.4-2.7			"serpentinized ultramafic rock"
13	A2	5N	15E	79AJC51	0.5			"amphibolite"
14	B6	7N	5E	79AJC71A	0.4-3.2		phyllite	wh mica+chl+qtz+opaq+plg+epi
15	C6	8N	5E	79AJC90	0.6-3.9		phyllite	wh mica+qtz+chl+opaq
16	D6	11N	4E	79AJC99	1.2-2.3			"hornblende-biotite granite"
17	D6	11N	4E	79AJC100	0.3			"hornblende-biotite granite"
18	D6	11N	4E	79AJC103	0.2-0.8			"hornblende-biotite granite"
19	D6	11N	4E	79AJC104	0.0-0.1			"hornblende-biotite granite" (contact zone)
20	B6	6N	5E	79AJC142	3.6			"schistose mgt musc quartzite
21	B5	7N	8E	79AWs78	$\leq$0.2	<0.025		"porphyritic rhyolite or rhyodacite"
22	B5	6N	7E	79AWr222	$\leq$0.2	<0.025		"porphyritic rhyolite or rhyodacite"
23	C6	11N	4E	79AWs75	0.8-1.1	2		"hornblende-biotite granite"
24	D4	12N	9E	79AJC146D	1.9-5.6	8.6		"gabbro"
25	D4	12N	9E	81AFr150	0.6-1.3	1.25		"amygdaloidal basalt"
26	C4	9N	8E	81ACA8	0.8-3.0			"calcareous musc amp chl qtz schist"
27	D4	12N	10E	81AWr105B	0.2-1.4			"basalt"
28	D4	12N	10E	81AWr106A	0.1-0.3			"spotty gabbro"
29	D4	12N	10E	81AWr107A	1.1-1.6			"basalt"
30	LIV D1	13N	3E	81ACA21A	3.3-8.5		metamafite	opaq+chl+wh mica+plg+carb+sphene
31	D6	12N	4E	81ACA25	0.5-1.3		quartzite	qtz+wh mica+chl+plg+opaq
32	D6	12N	5E	81ACA26	0.8-10.6			"serpentinite"
33	C4	10N	9E	81AWr151	12-22	26	altered peridotite?	mgt+trem+carb+serpentine
34	C4	10N	9E	81AWr152	0-50	200	altered peridotite?	carb+mgt+qtz+wh mica
35	C4	10N	9E	81AWr153	0.0			"nonmagnetic gabbro"

Table 1 (continued)

Map Number[1]	Quad	Twp.	Rng.	Field No.	Magnetic Susceptibility[2]	Remanent Magnetization[3]	Rock Name[4]	Thin section mineralogy or Field rock name[5]
36	D6	13N	4E	81AWr136	1.4		basalt	cpx+plg+ol
37	D2	11N	14E	81AFr253b	0.4-0.6			"dark grey-green basalt"
38	D2	11N	14E	81AFr254	0.0			"medium grained mafic intrusive rock"
39	B3	6N	11E	81AFr7113	0.7-3.3			"amphibolite and chloritic schist"
40	B2	6N	14E	79AFr401	1.7		pelitic schist	"qtz musc chl schist"
41	B1	6N	16E	79AFr419	2.1		pelitic schist	wh mica+qtz+chl+plg+opaq
42	B1	6N	16E	79AFr416	0.8		pelitic schist	wh mica+qtz+chl+plg+opaq
43	B3	6N	13E	79AWr344A	0.5		pelitic schist	wh mica+chl+qtz+plg+gar+opaq
44	C6	8N	4E	79AWr220	0.2-0.6			"chlorite qtz musc schist"
45	D2	12N	13E	81AFr223A	0.7			"mafic intrusive rock"
46	D2	12N	14E	81AFr224B	1.3			"mafic intrusive rock"
47	D6	11N	4E	79AFr411B	0.2-0.3			"ultramafic-carbonate rock"
48	A4	3N	9E	79AFr5052B	0.2			"mafic dike?"
49	B1	6N	16E	79AFr512A	1.0			"mgt chl musc quartzite"
50	A1	5N	18E	79AFr527C	0.4			"sulfide-bearing grey quartzite"
51	C1	9N	18E	82ACA430	0.4-1.4-2.4-10			"diabase, gabbro, and peridotite"
52	C1	10N	18E	82ACA439	0.0-0.4-1.3-6			"diorite, diabase, gabbro, and peridotite"
53	C1	10N	18E	82ACA447	1.2-2.3			"periodotite"
54	C1	10N	18E	81ACA57	0.0-0.6-5.3			"diorite, gabbro, and basalt"
55	C1	10N	18E	81ACA61	0.4-1.3			"gabbro and amygdaloidal basalt"
56	D1	11N	18E	82ACA452	0.0-0.3			"layered spotty gabbro"
57	A6	4N	5E	83AWr160A	0.0		altered ultramafic rock	amp+cpx
57	A6	4N	5E	83AWr160B	0.0		calc silicate rock	qtz+amp+plg+epi+gar+chl
57	A6	4N	5E	83AWr160C,D,E	0.0-2.2-2.9		serpentinite	serp+mgt

Notes:

1. Numbers 1-57 plotted beside dot for location on Plate 2.
2. Magnetic susceptibilities in units of 10^{-3} emu/cm^3 (e.g., 1.3 is 1.3×10^{-3} emu/cm^3). Multiple numbers indicate typical values measured. Susceptibility measured with portable field instrument with maximum sensitivity of 0.1×10^{-3} emu/cm^3.
3. Remanent magnetization in units of 10^{-3} emu/cm^3.
4. Rock name given in this column only for samples studied in thin section.
5. Thin section mineralogy by Jo Laird or George Snyder given without quotation marks in order of decreasing mode. If thin sections unavailable, field rock name given in quotation marks.

Table 1 (continued)

Abbreviations:

amp	amphibolite
bio	biotite
carb	carbonate
chl	chlorite
cpx	clinopyroxene
epi	epidote
gar	garnet
mgt	magnetite
opaq	opaque
plg	plagioclase
qtz	quartz
serp	serpentine
wh mica	white mica
musc	white mica, used in field rock name

CIRCLE, ALASKA

AERONAGNETIC AND BOUGUER GRAVITY MAP

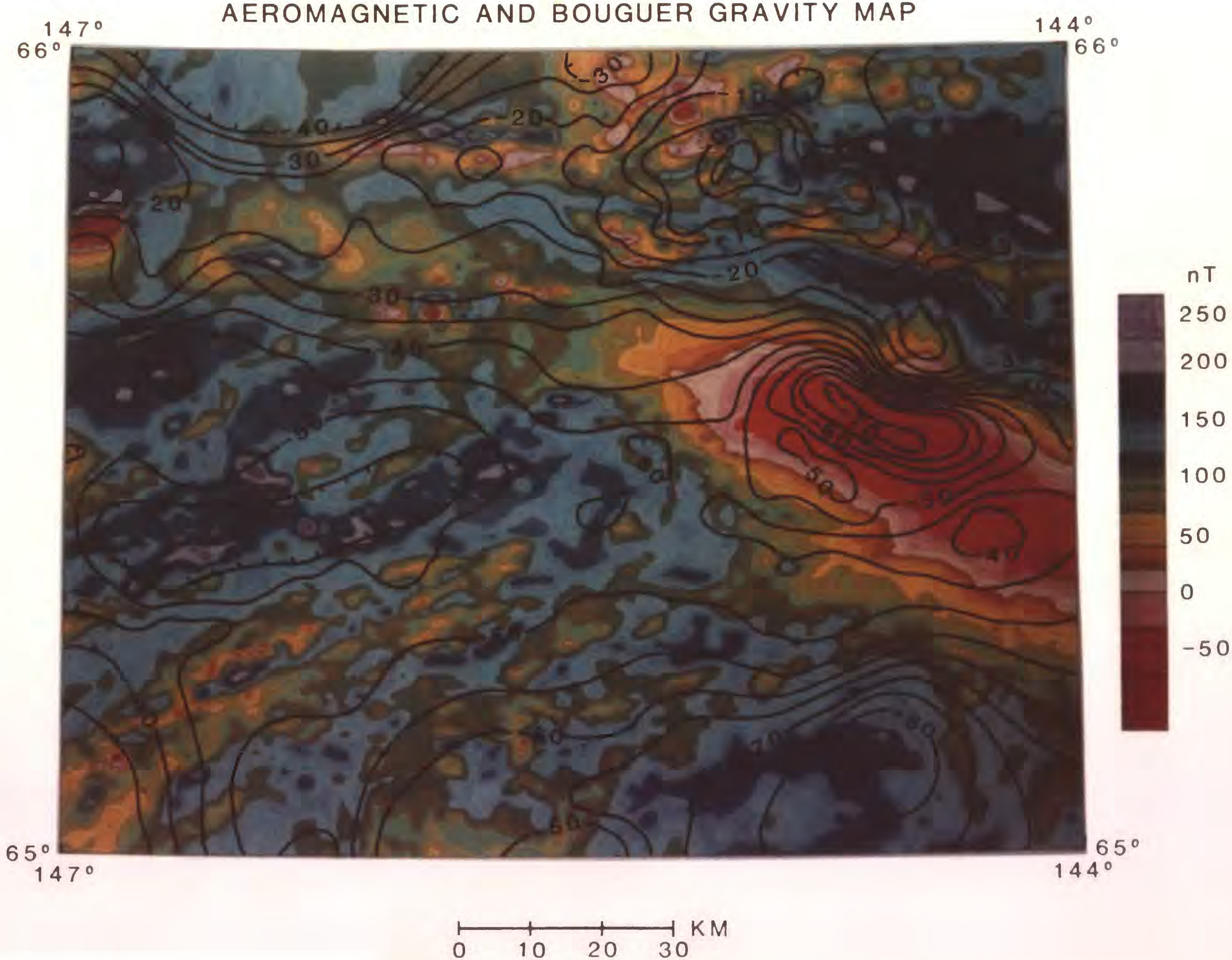

Figure 1

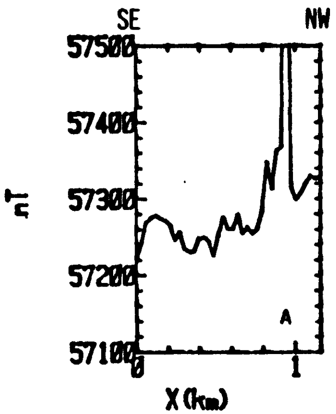

A. CIRCLE A-6. MAGNETIC GREENSCHIST (79AWR50) EXPOSED AT "A" CAUSES GROUND AND AEROMAGNETIC HIGHS.

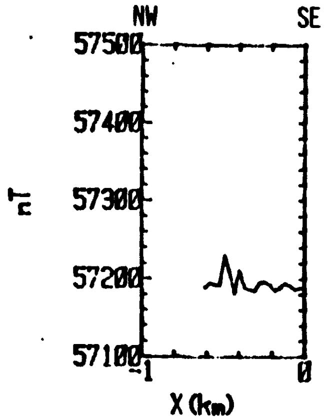

D. CIRCLE A-6. QUARTZITE EXPOSED. NO MAGNETIC ROCK FOUND.

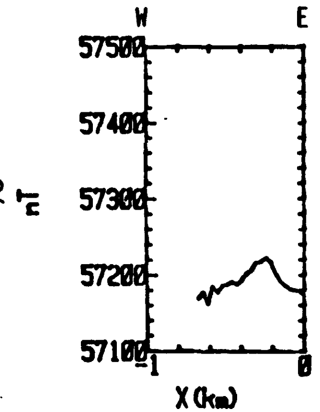

B. CIRCLE A-6. NONMAGNETIC QUARTZITE EXPOSED. MAGNETIC ROCKS NOT FOUND. SOURCE OF AEROMAGNETIC HIGH PROBABLY BURIED.

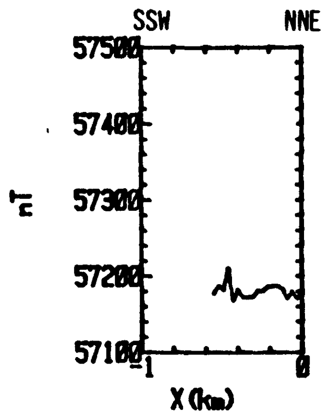

E. CIRCLE A-6. GARNETIFEROUS BIOTITE SCHIST EXPOSED. SOURCE OF AEROMAGNETIC HIGH NOT FOUND.

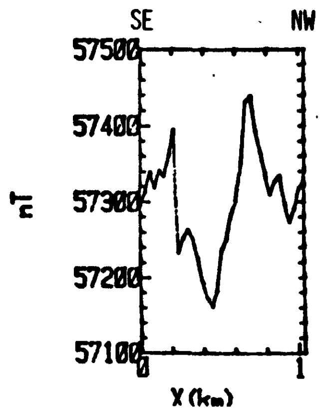

C. CIRCLE A-6. QUARTZITE, GRIT, AND SCHIST EXPOSED. SOURCE OF AEROMAGNETIC HIGH NOT FOUND, BUT IT MUST BE LESS THAN 100 METERS DEEP.

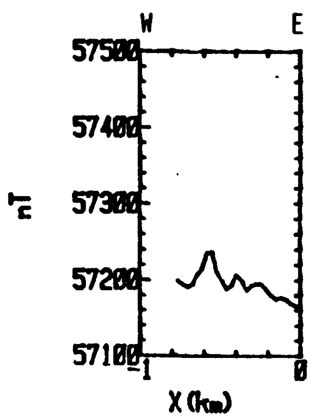

F. CIRCLE A-6. SCHIST AND QUARTZITE EXPOSED. SOURCE OF AEROMAGNETIC ANOMALY NOT FOUND.

Figure 2A - 2F

24

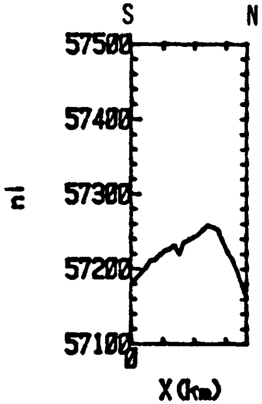

G. CIRCLE A-6. QUARTZITE EXPOSED. NO MAGNETIC ROCK FOUND. SOURCE OF AEROMAGNETIC HIGH BURIED.

H. (BELOW) CIRCLE A-6. QUARTZITE AND SCHIST EXPOSED. NO MAGNETIC ROCKS FOUND ON THIS TRAVERSE, BUT MAGNETIC CHLORITIC SCHIST FOUND 1 TO 2 KM TO EAST AND WEST. NARROW MAGNETIC HIGHS AT "A" AND "B" OCCUR IN FAULT ZONE CONTAINING CHLORITIC SCHIST.

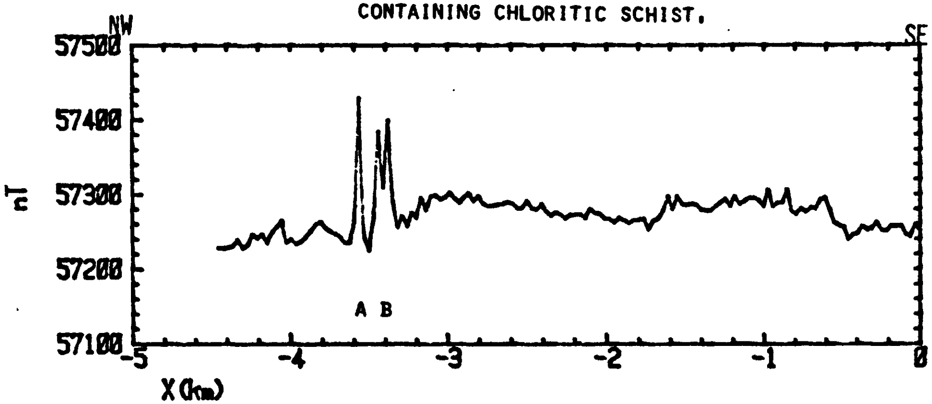

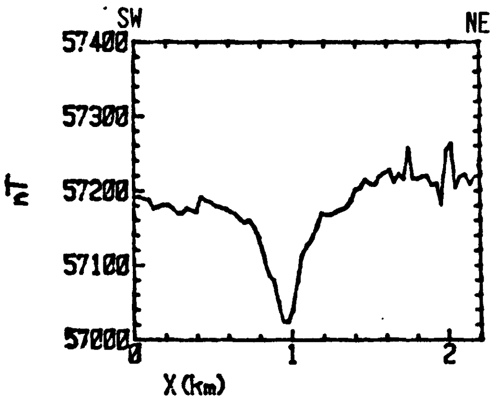

I. CIRCLE B-5. QUARTZITE EXPOSED, SOME CONTACT METAMORPHISM BY PLUTON. NARROW (400 M) 200 NT GROUND MAGNETIC LOW COINCIDES WITH 60 NT AEROMAGNETIC LOW, SUGGESTING THAT AEROMAGNETIC LOW IS CAUSED IN PART BY REVERSE REMANENT MAGNETIZATION.

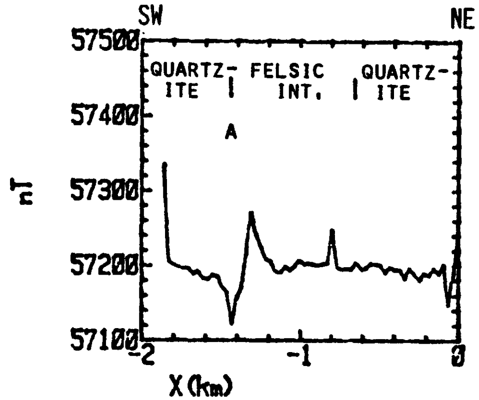

J. CIRCLE B-5. MAGNETIC TRAVERSE OVER FELSIC HYPABYSSAL INTRUSIVE IN QUARTZITE SHOWS NO SUSCEPTIBILITY CONTRAST BETWEEN UNITS. THERE MAY BE MAGNETIC ROCKS IN THE SOUTHWESTERN CONTACT ZONE AT "A".

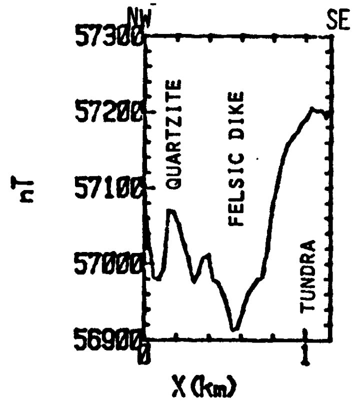

K. CIRCLE B-5. NARROW (200 M) GROUND MAGNETIC LOW AT FELSIC DIKE COINCIDES WITH 110 NT AEROMAGNETIC LOW. REVERSE REMANENT MAGNETIZATION ASSOCIATED WITH DIKE OR CONTACT METAMORPHIC ROCK IS INFERRED TO BE THE CAUSE OF THE AEROMAGNETIC LOW.

L. (BELOW) CIRCLE D-6. HIGH MAGNETIC RELIEF OVER MAGNETIC HORNBLENDE-BIOTITE GRANITE OF VICTORIA MOUNTAIN. NOTE ABRUPT TRANSITION TO NONMAGNETIC ROCKS AT NORTHERN CONTACT OF PLUTON, COMPARED TO VARIABLY-MAGNETIC CONTACT ROCKS SOUTH OF PLUTON.

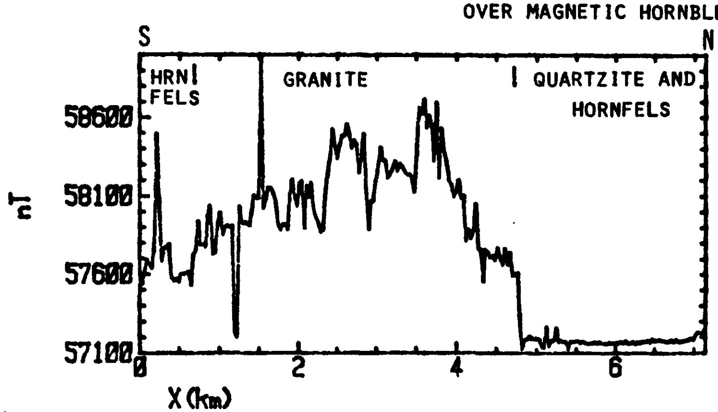

Figure 2G - 2L

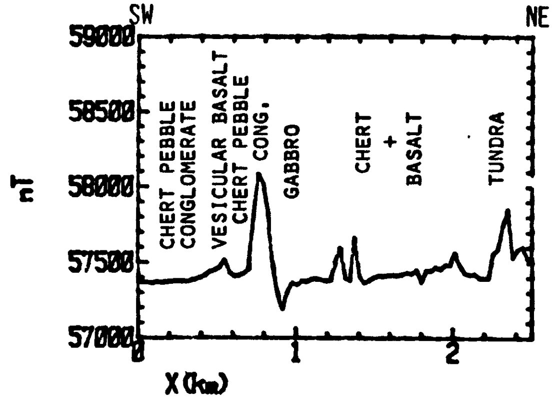

M. CIRCLE D-4.
NARROW (200 M) MAGNETIC HIGH OVER CHERT PEBBLE CONGLOMERATE CAUSED BY UNDERLYING OR ADJACENT GABBRO.

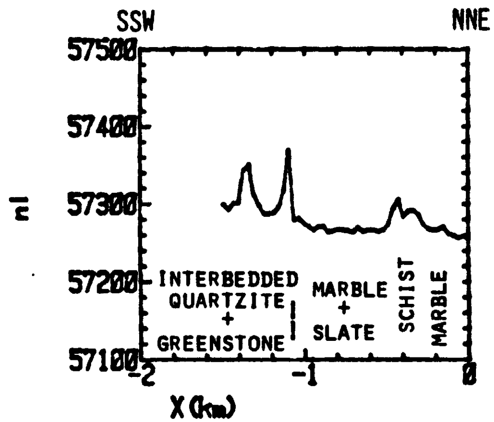

P. CIRCLE D-6.
MAGNETIC HIGH CAUSED BY MAGNETIC GREENSTONE INTERBEDDED WITH QUARTZITE.

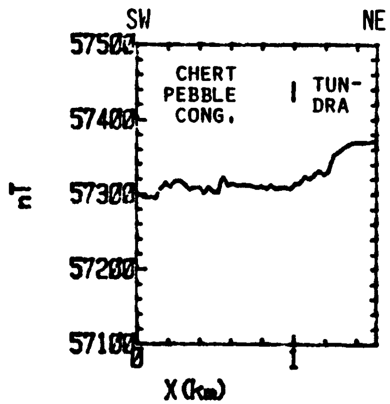

N. CIRCLE D-4. STEP TO HIGHER MAGNETIC VALUES IN NORTHEAST MARKS HIDDEN CONTACT BETWEEN CHERT PEBBLE CONGLOMERATE AND INFERRED MAGNETIC BASALT OR GABBRO. MAGNETIC ROCK NOT FOUND.

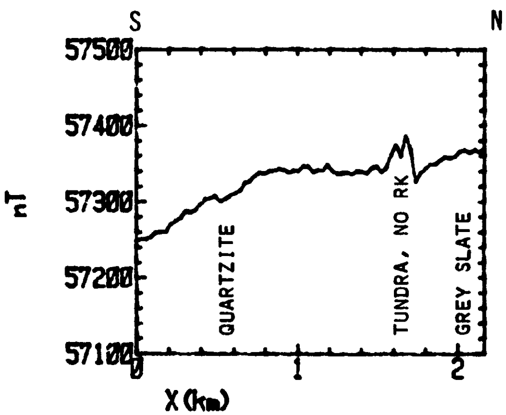

Q. CIRCLE D-5.
GROUND MAGNETIC PROFILE SHOWS APPROXIMATELY SAME TOTAL RELIEF (115 nT) AS AEROMAGNETIC HIGH. NO MAGNETIC ROCK FOUND. MAGNETIC SOURCE IS MAINLY BURIED BY QUARTZITE, BUT SOME MAGNETIC ROCK OCCURS CLOSE TO SURFACE IN TUNDRA-COVERED AREAS.

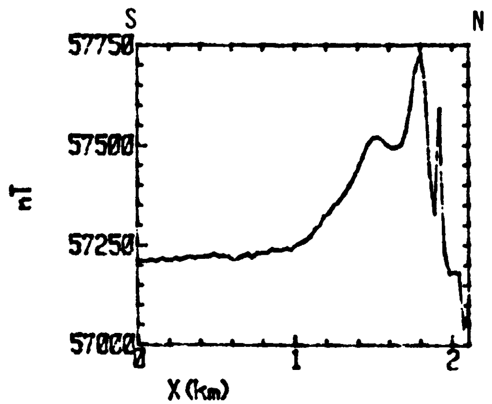

O. LIVENGOOD D-1 NEAR CIRCLE D-6 BORDER. MAGNETIC HIGH CAUSED BY MAFIC INTRUSIVE IN LIMESTONE, SUBSEQUENTLY DYNATHERMALLY METAMORPHOSED.

Figure 2M - 2Q

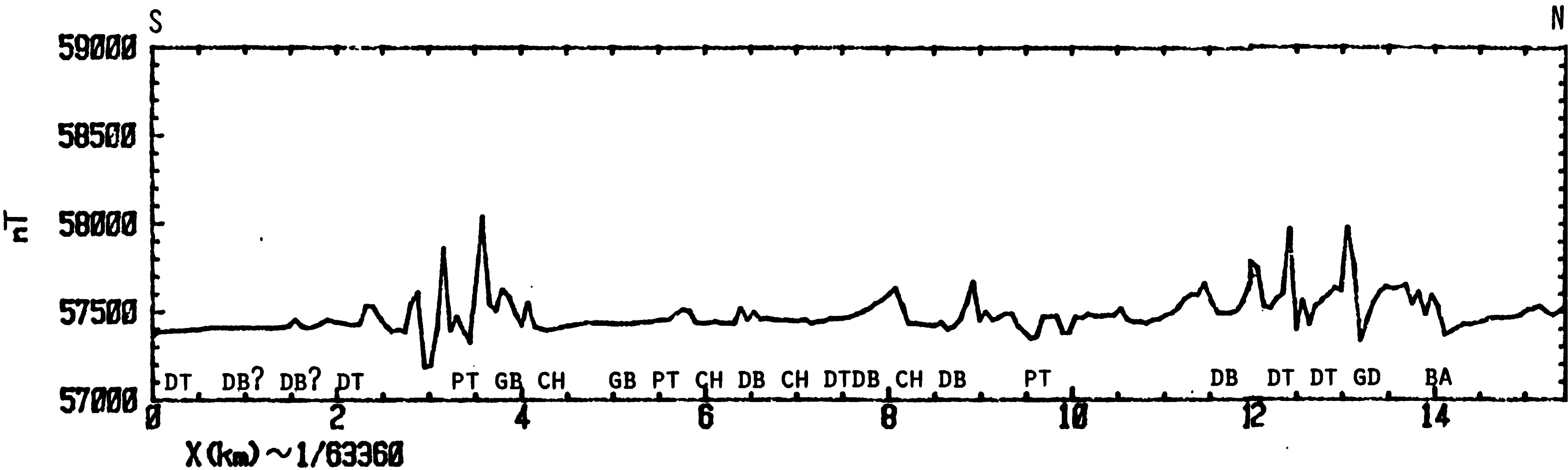

R. CIRCLE C-1. MAGNETOMETER TRAVERSE MADE ON BOAT IN YUKON RIVER. MANY AEROMAGNETIC HIGHS AND SURFACE MAGNETIC HIGHS OBSERVED IN RIVER ARE ASSOCIATED WITH PERIDOTITE AND GABBRO. IN TWO CASES WHERE MAGNETIC PERIDOTITE OCCURS ON SHORE (LABELED PT), NO MAGNETIC HIGH OCCURS IN RIVER, CONFIRMING AEROMAGNETIC INTERPRETATION THAT EAST-WEST TRENDING PERIDOTITE LAYERS ARE TRUNCATED AT THE RIVER, POSSIBLY BY A FAULT.

Figure 2R

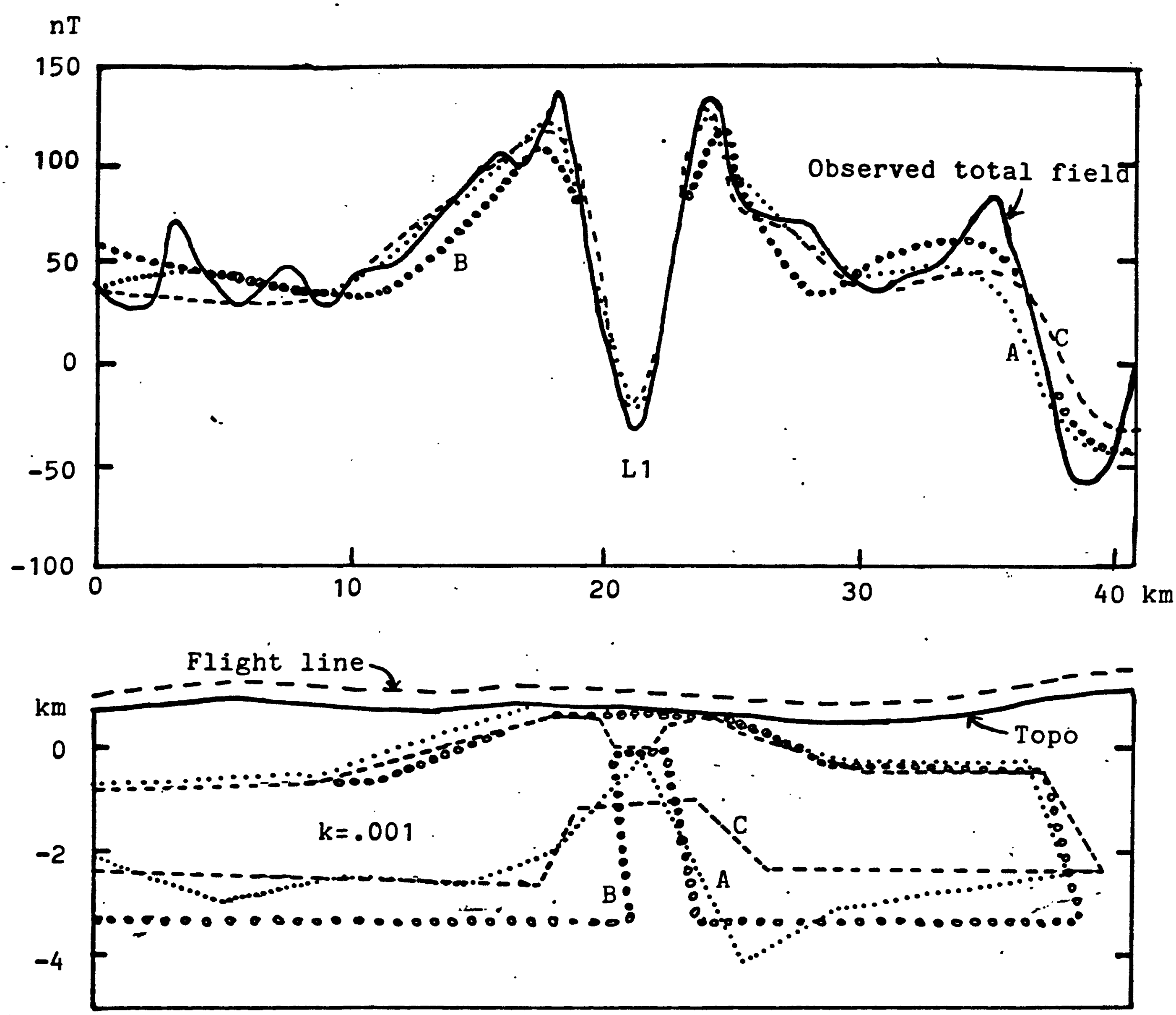
nT
150
100
50
0
-50
-100
Observed total field
B
A
C
L1
0
10
20
30
40 km
Flight line
km
0
-2
-4
Topo
k=.001
C
A
B

Figure 3.

Figure 4.

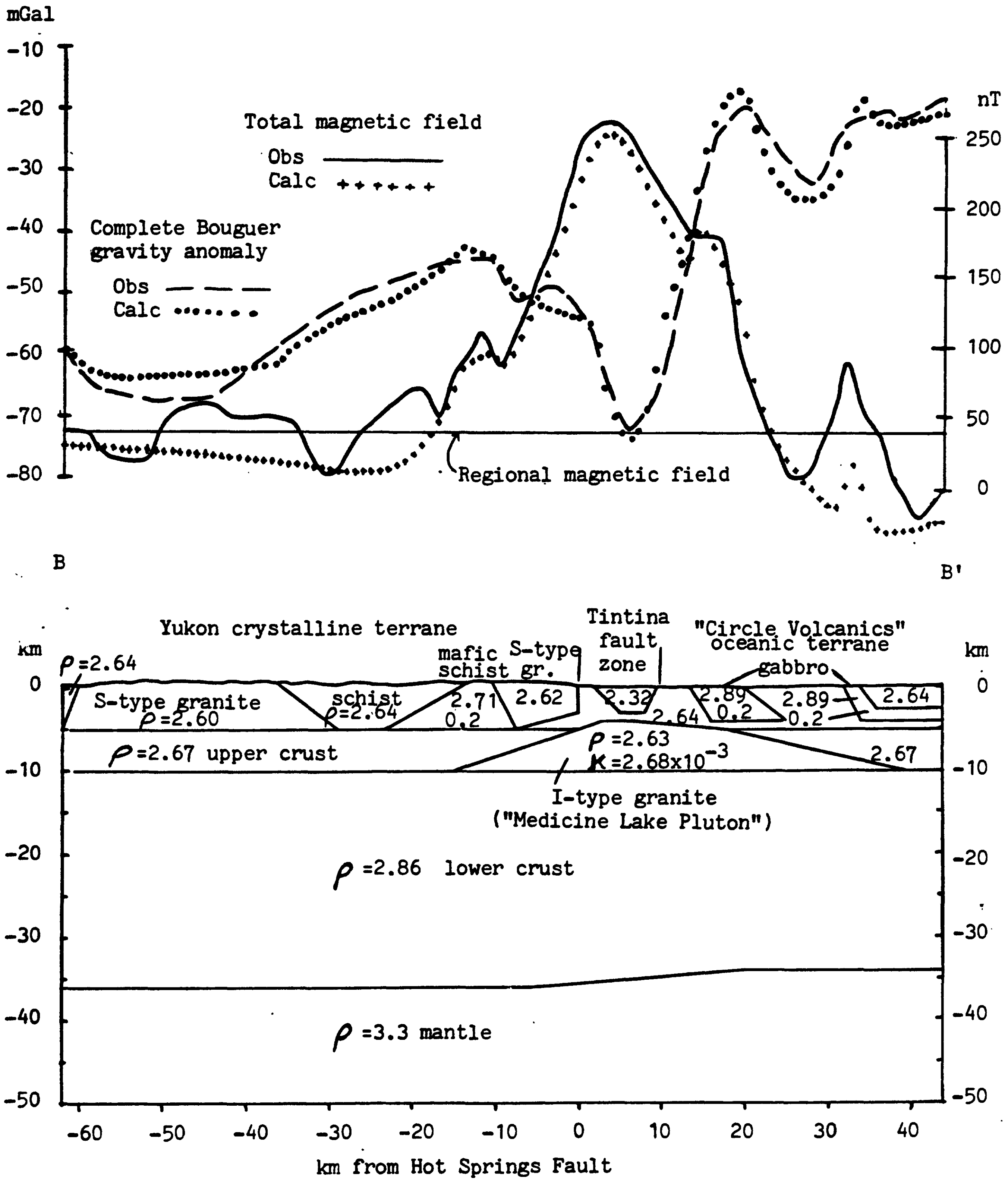

mGal
-10
-20
-30
-40
-50
-60
-70
-80
Total magnetic field
Obs
Calc
Complete Bouguer gravity anomaly
Obs
Calc
nT
250
200
150
100
50
0
Regional magnetic field
B
B'
Yukon crystalline terrane
Tintina fault zone
"Circle Volcanics" oceanic terrane
km
ρ=2.64
mafic schist
S-type gr.
gabbro
0
S-type granite ρ=2.60
schist ρ=2.64
2.71 0.2
2.62
2.32
2.64
2.89 0.2
2.89 0.2
2.64
ρ=2.67 upper crust
ρ=2.63 K=2.68x10^-3
2.67
-10
I-type granite ("Medicine Lake Pluton")
-20
ρ=2.86 lower crust
-30
-40
ρ=3.3 mantle
-50
-60 -50 -40 -30 -20 -10 0 10 20 30 40
km from Hot Springs Fault